Contribution of vegetation and peat fires to particulate air pollution in Southeast Asia

C L Reddington[1], M Yoshioka[1], R Balasubramanian[2], D Ridley[3], Y Y Toh[4], S R Arnold[1] and D V Spracklen[1]

[1]Institute for Climate and Atmospheric Science, School of Earth and Environment, University of Leeds, UK
[2]Department of Civil and Environmental Engineering, National University of Singapore, Singapore
[3]Department of Civil and Environmental Engineering, Massachusetts Institute of Technology, USA
[4]Environmental Studies Division, Malaysian Meteorological Department, Malaysia

Supplementary Material

METHODS

1. Global aerosol model

1.1 Model description

The global distribution of aerosol was simulated using the 3-D Global Model of Aerosol Processes (GLOMAP; Spracklen et al., 2005; Mann et al., 2010), which is an extension to the TOMCAT chemical transport model (Chipperfield, 2006). TOMCAT is driven by analysed meteorology from the European Centre for Medium Range Weather Forecasts (ECMWF), updated every 6 hours and linearly interpolated onto the model time-step. Model output has a horizontal resolution of 2.8˚×2.8˚ and 31 vertical model levels between the surface and 10 hPa. The vertical resolution in the boundary layer ranges from ~60 m near the surface to ~400 m at ~2 km above the surface.

GLOMAP simulates the mass and number of size resolved aerosol particles in the atmosphere, including the influence of aerosol microphysical processes on the particle size distribution. These processes include nucleation, coagulation, condensation, cloud processing, dry deposition, and nucleation/impact scavenging. The aerosol particle size distribution is represented using seven log-normal modes (Mann et al., 2010). GLOMAP treats black carbon (BC), particulate organic matter (POM), sulfate (SO_4), sea spray and mineral dust. Here we specify concentrations of oxidants using monthly-mean 3-D fields at 6-hourly intervals from a TOMCAT simulation with detailed tropospheric chemistry (Arnold et al., 2005) linearly interpolated onto the model time-step.

For anthropogenic emissions of sulfur dioxide (SO_2), BC and POM we use the MACCity emissions inventory (Lamarque et al., 2010), which provides annually-varying monthly-mean emissions for the period 1979–2010. For simulations in the year 2011 we used MACCity anthropogenic emissions from 2010. Biomass burning emissions of SO_2, BC and POM are based on the Global Fire Emissions Database (GFED; van der Werf et al. 2004; 2006; 2010) and are described in Section S3. The injection heights of the fire emissions were distributed over six ecosystem-dependent altitudes between the surface and 6 km recommended by Dentener et al. (2006). In the region studied in this paper, fire emissions are injected between the surface and an altitude of 1000 m asl. Over Sumatra and eastern Kalimantan ~90-95% of fire emissions are injected between the surface and 500 m asl, with the remaining ~5-10% injected between 500 and 1000 m asl. Over western Kalimantan and Malaysian Borneo, ~65-70% of fire emissions are injected between the surface and 500 m asl, with ~30-35% emitted above 500 m asl. Our assumed injection heights are consistent with satellite retrieved fire plumes from Borneo and Sumatra, with the majority of plumes at a height of between ~300 and ~1100 m (Tosca et al., 2011).

1.2 Calculation of aerosol optical depth

We calculate aerosol optical depth (AOD) at 440 nm from the global model output using Mie theory assuming spherical particles (Grainger et al., 2004) and aerosol refractive indices following Bellouin et al. (2011), treating aerosol as externally mixed within each log-normal mode. Water uptake plays a significant role in determining AOD, altering the refractive index and the size distribution of the aerosol mixture. The water uptake for each soluble aerosol component is calculated on-line in the model according to ZSR theory (Stokes and Robinson, 1966; see Mann et al., 2010) and the resulting daily-mean wet radii and refractive indices used to calculate the daily-mean aerosol extinction.

2. Atmospheric back trajectories

We used the ROTRAJ (Reading Offline Trajectory model) Lagrangian transport model (Methven et al, 2003) to calculate five-day atmospheric back-trajectories arriving at Singapore (1.37˚N, 103.75˚E) every six hours (0, 6, 12, 18 hours UTC) for the period January 2004 to December 2007. Trajectories were initialised on a hybrid sigma-pressure coordinate of 0.99, just above the surface. The simulations utilise velocity fields taken from ECMWF operational analyses. The fields at the Lagrangian particle positions are obtained from the 1.0125º horizontal resolution analyses by cubic Lagrange interpolation in the vertical followed by bilinear interpolation in the horizontal direction. These trajectories account for large-scale advection by the resolved winds but do not account for sub-grid convective and turbulent transport.

We calculated the cumulative exposure of air masses to fire emissions over the five days of atmospheric transport to Singapore. We assumed that air masses are exposed to fire emissions when they are within the well-mixed boundary layer, here specified as when atmospheric pressure of the air mass is within 150 hPa of the surface pressure. We linearly interpolated the location of the air mass every 15 minutes (from the 6 hourly positions). At each location we used bilinear interpolation onto the nearby grid points from the emission dataset to calculate fire emission into the air mass. The methodology is described in detail in Arnold et al. (2010).

3. Fire emissions

Fire emissions were taken from the GFED version 3 emission inventory (GFED3; van der Werf et al., 2010). GFED3 provides yearly-varying, monthly-mean fire emissions of aerosol and gas-phase species from 1997 to 2011 at 0.5º×0.5º resolution (van der Werf et al., 2010). The global emissions are derived using estimates of burnt area, active fire detections, and plant productivity from the Moderate resolution Imaging Spectroradiometer (MODIS) satellite (post year 2000) combined with estimates of fuel loads and combustion completeness for each monthly time step from the Carnegie-Ames-Stanford-Approach (CASA) biogeochemical model. The monthly-mean GFED3 emissions of BC, POM and SO_2 were implemented in the GLOMAP model for the period 2000–2011. The ROTRAJ model simulations used GFED3 emissions of carbon monoxide (CO) for the period 2004–2007.

For comparison, we also applied fire emissions from the National Centre for Atmospheric Research Fire Inventory (FINNv1; Wiedinmyer et al., 2011) into the GLOMAP model. FINNv1 provides yearly varying, daily emissions from 2002 to 2012 on a 1 km^2 grid. FINNv1 fire emissions are calculated from MODIS active fire detections, which are used to estimate burnt area (assuming an area of 0.75-1 km^2 for each fire count). Burnt area is converted to emissions using fuel load estimates and emission

factors from the literature. The active fire product used by FINNv1 is more sensitive to small fires than the burnt area product used by GFED3, which means that in regions dominated by small fires e.g. agricultural areas, FINNv1 emissions are likely to be higher than GFED3.

Previous work has compared GFED3 against FINNv1 emissions of CO over Southeast Asia. Whilst FINNv1 fire emissions are larger than GFED3 over much of Southeast Asia, FINNv1 emissions are several times smaller for tropical peat fires (Andela et al., 2013). The representation of peat fire emissions in GFED3 may be superior relative to FINNv1 because the peatlands in Sumatra and Borneo were included separately into the GFED3 biome map (van der Werf et al., 2010) using the Terrestrial Ecoregions of the World map (Olson et al., 2001).

4. Observations

To evaluate the distribution of particulate matter with diameters less than 2.5 μm ($PM_{2.5}$) simulated by GLOMAP, we used in-situ measurements of daily-mean $PM_{2.5}$ conducted at the Atmospheric Research Station, National University of Singapore (103.780ºE, 1.298ºN), using an annular denuder system (URG, Inc., USA) (Balasubramanian et al., 2003). We also used measurements of particulate matter with diameters less than 10 μm (PM_{10}) conducted at the Global Atmosphere Watch (GAW) stations in Petaling Jaya (located in Selangor, Peninsular Malaysia), Danum Valley (located in Sabah, Malaysian Borneo) and Bukit Kototabang (located in West Sumatra, Sumatra). The geographical locations of these measurement sites are shown in Figure 1 and summarised in Table S1. The PM_{10} measurements were made using three different instruments: a high-volume aerosol sampler at Petaling Jaya; a Tapered Element Oscillating Microbalance (TEOM) system (Rupprecht and Patashnick Co. Inc.) at Danum Valley; and a Beta-ray Attenuation Mass Monitor BAM-1020 (MetOne Inc., USA) at Bukit Kototabang. Daily-mean PM_{10} concentrations were provided from Petaling Jaya and Danum Valley and hourly-mean PM_{10} concentrations were provided from Bukit Kototabang. The length of observation period varies by site and is summarised in Table S1. At sites where the observation period extends beyond the period focused on in our study (2004-2009) (Bukit Kototabang and Petaling Jaya), we restricted the model-observation comparisons to within the studied time frame. Prior to comparison with observations, the simulated daily-mean $PM_{2.5}$ or PM_{10} concentration was interpolated to the location (latitude, longitude and altitude above sea level) of each measurement station.

We also evaluate the model against aerosol optical depth (AOD) recorded by 13 stations in the Aerosol Robotic Network (AERONET), located across Southeast Asia. We used data from stations that have Level 2 daily-mean AOD data available for at least one year within the time period of available GFED3 fire emissions data (1997–2011). The locations of these AERONET stations are shown in Figure 1 and Table S1. As for comparisons with PM, the simulated daily-mean AOD was interpolated to the location (latitude, longitude and altitude above sea level) of each AERONET station. The length of observation period again varies by site and is also summarised in Table S1. The AERONET Level 2 product includes automatic cloud screening, which leads to missing-data gaps in the daily-mean AOD data. Days corresponding to these gaps were removed from the modelled daily-mean AOD before calculating the monthly-mean values used in the analysis. Because of the relatively frequent gaps in the AOD dataset, we did not restrict the model-observation comparisons of AOD to within the period analysed in our study (2004-2009), so to utilise as much AOD data as possible.

We note that whilst the majority of cloud-contaminated AOD data is removed in the AERONET Level 2 data; comparisons with co-located Micro-Pulse Lidar Network (MPLNET) observations indicate that some contamination from thin cirrus clouds may remain in data recorded in Southeast Asia (Huang et al., 2011; Chew et al., 2011). These contaminations can lead to a positive bias in the

observed monthly-mean AOD of ~5% at the Pimai station in Thailand (Huang et al., 2011) and ~0.03–0.06 in Singapore (Chew et al., 2011). The biases at other stations in Southeast Asia have not yet been quantified.

Station	Country	Observation period	Geographical position	Location classification	PI or reference
Singapore ($PM_{2.5}$)	Singapore	01/01/00 – 31/12/00	103.78^{0}E, 1.2977^{0}N	Urban, city centre	Balasubramanian et al. (2003)
Petaling Jaya (PM_{10})	Malaysia	01/01/06 – 31/12/09	101.65^{0}E, 3.1^{0}N	Urban, city centre	Maznorizan Mohamad, Toh Ying Ying and Siti Hawa Shuhami
Bukit Kototabang (PM_{10})	Indonesia	01/01/04 – 31/12/09	100.32^{0}E, 0.2019^{0}S	Rural/tropical forest	Ilahi and Nurhayati (2012)
Danum Valley (PM_{10})	Malaysia	01/01/11 – 31/12/11	117.84^{0}E, 4.9814^{0}N	Pristine tropical rainforest	Maznorizan Mohamad, Toh Ying Ying, Thomas Tuch and Alfred Wiedensohler
Singapore (AERONET)	Singapore	14/11/06 – 19/10/12	103.78^{0}E, 1.2977^{0}N	Urban, city centre	Soo-Chin Liew and Santo V. Salinas Cortijo
ND Marbel Univ. (AERONET)	Rep. of the Philippines	17/12/09 – 19/01/12	124.84^{0}E, 6.4960^{0}N	Urban, city centre	Susana Dorado
Songkhla Met. Station (AERONET)	Thailand	11/01/07 – 13/12/11	100.61^{0}E, 7.1844^{0}N	Urban, city centre	Serm Janjai
Bandung (AERONET)	Indonesia	13/05/09 – 28/09/11	107.61^{0}E, 6.888^{0}N	Urban, city centre	Puji Lestari and Brent Holben
Chulalongkorn (AERONET)	Thailand	19/02/03 – 25/09/04	100.53^{0}E, 13.736^{0}N	Urban, city centre	Brent Holben
Ubon Ratchathani (AERONET)	Thailand	09/10/09 – 07/11/12	104.87^{0}E, 15.246^{0}N	Urban, within city limits	Serm Janjai
Manila Observatory (AERONET)	Rep. of the Philippines	21/01/09 – 30/12/11	121.08^{0}E, 14.635^{0}N	Urban, within city limits	Nofel Lagrosas and Brent Holben
Silpakorn University (AERONET)	Thailand	15/08/06 – 11/12/11	100.04^{0}E, 13.819^{0}N	Urban, city outskirts	Serm Janjai
Chiang Mai Met. Station (AERONET)	Thailand	17/09/06 – 28/07/11	98.973^{0}E, 18.771^{0}N	Urban, city outskirts	Serm Janjai
Bac Giang (AERONET)	Vietnam	03/03/03 – 26/12/09	106.23^{0}E, 21.291^{0}N	Rural, city outskirts	Nguyen Xuan Anh
Bac Lieu (AERONET)	Vietnam	10/03/03 – 25/04/11	105.73^{0}E, 9.2800^{0}N	Rural, city outskirts	Nguyen Xuan Anh
Mukdahan (AERONET)	Thailand	07/11/03 – 30/05/10	104.68^{0}E, 16.607^{0}N	Rural	Brent Holben
Phimai (AERONET)	Thailand	18/02/03 – 10/04/08	102.56^{0}E, 15.182^{0}N	Rural	Brent Holben

Table S1. Summary of the AERONET and particulate matter (PM) measurement stations used to evaluate modelled AOD and PM over Southeast Asia. The Principal Investigator(s) (PI) responsible for each dataset (or the data reference if available) are shown in the final column.

RESULTS

5. Inter-annual variability in contributions of fires to $PM_{2.5}$

Figure S1 shows monthly-mean $PM_{2.5}$ concentrations in Singapore simulated by GLOMAP over the period January 2004 to December 2009. Figure S1 shows that the inter-annual variability in simulated $PM_{2.5}$ is driven by strong inter-annual variability in fire emissions across Southeast Asia. The inter-annual variability in fire emissions in this region is linked to the effects of El Niño Southern

Oscillation (ENSO) and the Indian Ocean Dipole (Saji et al., 1999) on the meteorological conditions (particularly precipitation and prevailing wind pattern) over Southeast Asia, as discussed in the main text.

Simulated $PM_{2.5}$ concentrations vary substantially from year to year, with the largest concentrations occurring during 2006, towards the end of the dry season (August-October). This large peak in $PM_{2.5}$ above the background concentration (of ~10 μg m^{-3}) is due to emissions from fires, with fires in southern Sumatra and Indonesian Borneo making the largest contributions (37.6 μg m^{-3} and 17.3 μg m^{-3} in October, respectively). These results are consistent with an observational study by Engling et al. (2014). Large increases in $PM_{2.5}$ due to fire emissions also occur during August-October in 2004 and 2009, with maximum increases in September of 15.8 μg m^{-3} and 12.0 μg m^{-3}, respectively. Fires located in southern Sumatra are mostly responsible for these increases in simulated $PM_{2.5}$, contributing 11.4 μg m^{-3} and 9.8 μg m^{-3} in September of 2004 and 2009, respectively. In 2004, 2005, 2006 and 2009 fires in central Sumatra contribute considerably to $PM_{2.5}$ earlier in the year (between February and August). This is particularly evident in 2005, where fires in central Sumatra make the largest contribution of the eight regions to $PM_{2.5}$ in Singapore, peaking in February (14.8 μg m^{-3}).

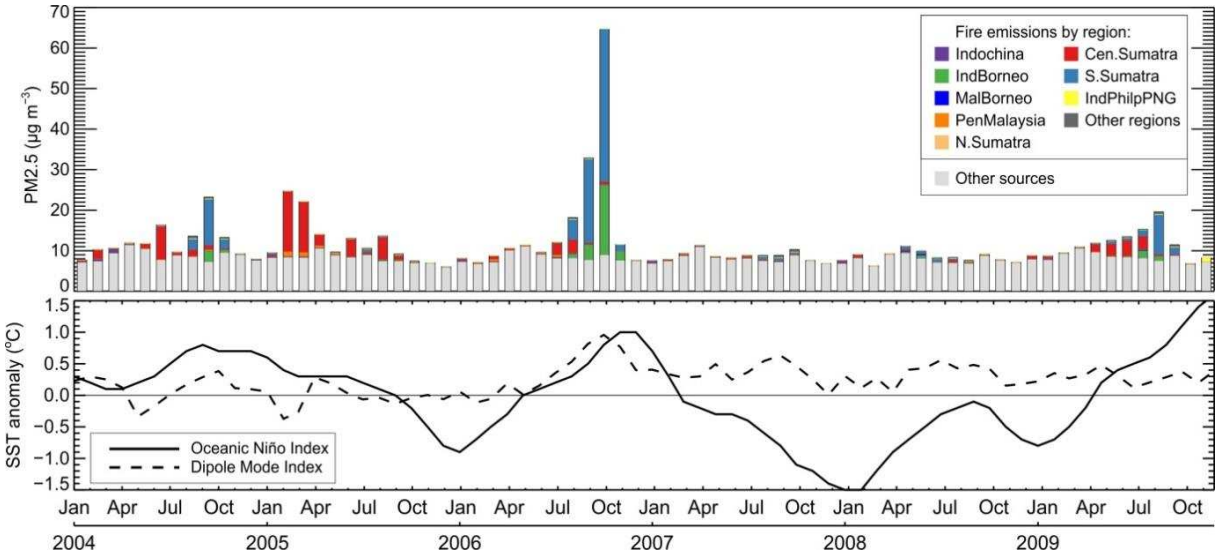

Figure S1. Upper panel: Simulated monthly-mean $PM_{2.5}$ concentrations over Singapore for the period January 2004 to December 2009. The coloured sections of the bars indicate the absolute contribution from fires in different regions (defined in Figure 1) to monthly-mean $PM_{2.5}$. The light grey sections indicate contributions to $PM_{2.5}$ from other sources (e.g. natural emissions, fossil/bio fuel emissions etc.). Lower panel: Time-series of the monthly Oceanic Niño Index[1] (ONI; which indicates the strength and sign of ENSO) and Dipole Mode Index[2] (DMI; which indicates the strength and sign of the Indian Ocean Dipole) for the 2004-2009 period. The ONI is a 3-month running mean of ERSST.v3b sea surface temperature (SST) anomalies in the Niño 3.4 region (5ºN-5ºS, 120º-170ºW), based on centred 30-year base periods updated every 5 years. The DMI (Saji et al., 1999) is an anomalous SST gradient between the western equatorial Indian Ocean (50ºE-70ºE and 10ºS-10ºN) and the south eastern equatorial Indian Ocean (90ºE-110ºE and 10ºS-0ºN).

[1]http://www.cpc.noaa.gov/products/analysis_monitoring/ensostuff/ensoyears.shtml

[2]http://www.jamstec.go.jp/frsgc/research/d1/iod/iod/dipole_mode_index.html

6. Spatial distribution of enhancements to $PM_{2.5}$ from fires

Figure S2 shows the spatial distribution of the enhancement from fires in different regions to annual (2006) mean $PM_{2.5}$ concentrations simulated by GLOMAP over Southeast Asia. Figure S2 shows that

enhancements to the local annual-mean $PM_{2.5}$ concentrations from fires in Indochina is considerable (up to ~5 μg m^{-3}) over a large region. However, because of the prevailing wind pattern in that year there is little or no impact on annual-mean $PM_{2.5}$ concentrations in Singapore. On the other hand, although the enhancement to local annual-mean $PM_{2.5}$ from fires in central Sumatra is of a similar magnitude to the enhancement from fires in Indochina (over a smaller area); the impact on $PM_{2.5}$ concentrations in Singapore is greater because of the proximity of the fires to Singapore and the prevailing wind direction during a large part of the year.

The simulated enhancement to annual-mean $PM_{2.5}$ from fires in southern Sumatra and Indonesian Borneo is substantial over Singapore and the surrounding regions in 2006 (increasing annual mean concentrations by up to ~15 μg m^{-3}). This large enhancement simulated by the model is due to a combination of the high smoke emission fluxes in these regions, the prevailing wind patterns that transport these emissions over Singapore and the reduction in rainfall (i.e. removal of aerosol) resulting from positive El Niño and IOD conditions (Figure S1). We note that due to the considerable inter-annual variability in fires occurring across Southeast Asia (discussed above), the enhancements to annual-mean $PM_{2.5}$ concentrations from fires shown in Figure S2 (for 2006) are likely to be at the upper end of air quality impacts of fires during the study period (2004-2009).

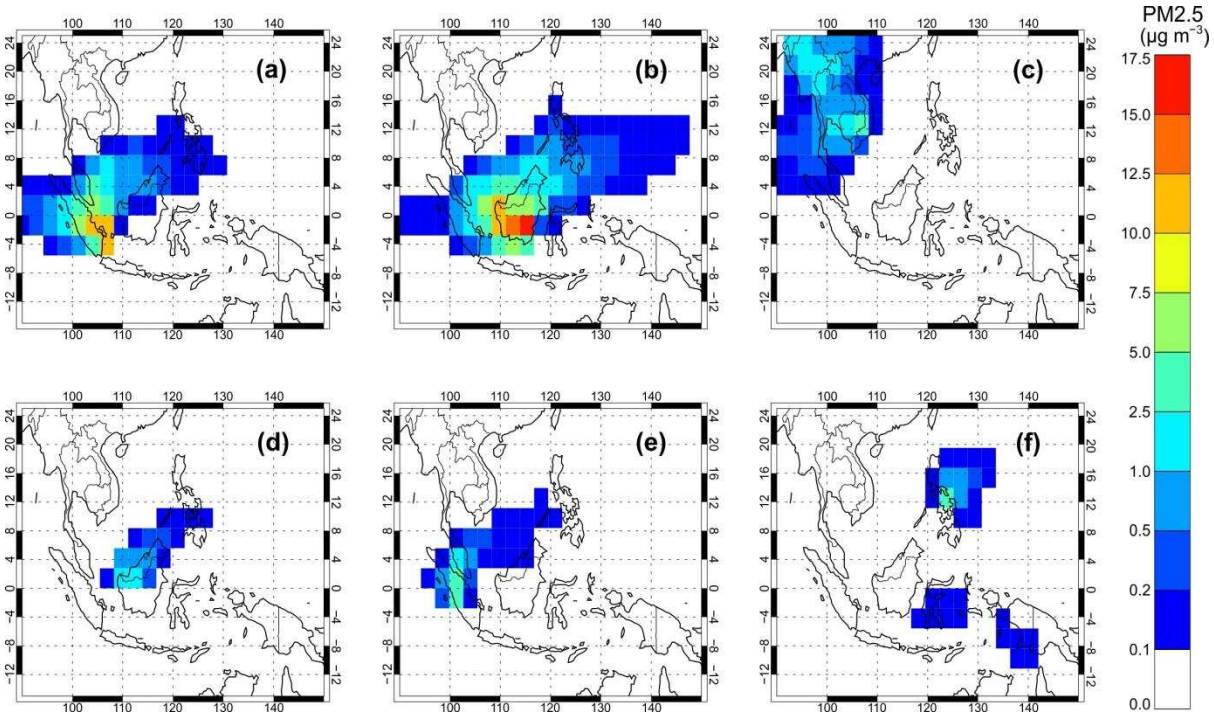

Figure S2. Spatial distribution of the enhancement to 2006 annual-mean $PM_{2.5}$ concentrations simulated by GLOMAP from fires in **(a)** southern Sumatra, **(b)** Indonesian Borneo (Kalimantan), **(c)** Indochina (Thailand, Cambodia, Vietnam, Laos, and Myanmar), **(d)** Malaysian Borneo, **(e)** central Sumatra and **(f)** Indonesia (excluding Sumatra and Kalimantan), Philippines and Papua New Guinea. Regions are displayed in Figure 1. Annual mean $PM_{2.5}$ concentrations are displayed on the native grid of GLOMAP (2.8˚ by 2.8˚).

7. Seasonal variability in transported fire emissions

Figure S3 shows five-day atmospheric back trajectories, simulated by ROTRAJ, arriving in Singapore for the year 2006. There is a strong seasonal cycle in the prevailing wind patterns near the surface over Singapore and surrounding areas. During ~December–March (the Northeast Monsoon season),

the prevailing wind is from the northeast with back trajectories mainly passing over the sea. During ~April–May, the prevailing wind direction transitions from predominantly northeasterly to predominantly southeasterly. During ~June–October (the Southwest Monsoon season) the prevailing wind is from the southeast, transporting fire emissions from southern Sumatra and southern and western Kalimantan. Early on in this period (in June) the wind occasionally comes from a south and southwest direction, transporting fire emissions from central Sumatra. These patterns match atmospheric transport patterns reported by Xian et al. (2013).

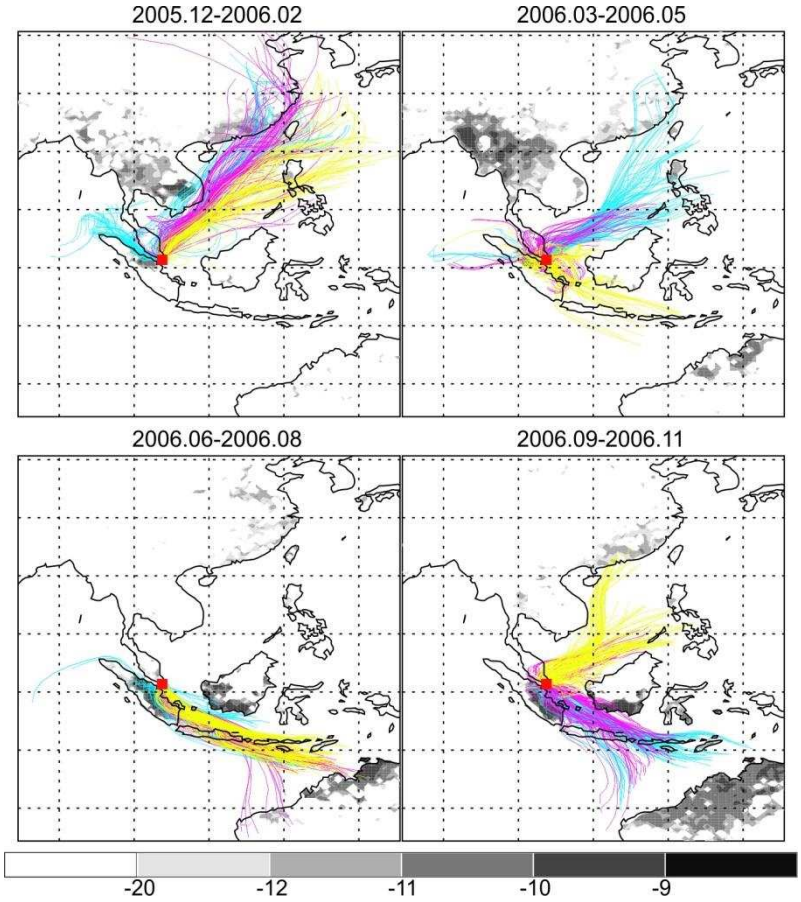

Figure S3. Five-day atmospheric back-trajectories arriving in Singapore for 3-month periods from December 2005 to November 2006. Trajectories of the first, second and third month in each period are shown in cyan, magenta and yellow respectively. Three-month mean GFED3 fire emissions of CO for 2006 are shown by grey shading (units are in kg(CO) m^{-2} s^{-1} with scales showing the common logarithm values).

Figure S3 indicates that the seasonal change in regions contributing to Singapore air quality occurs due to the changes in both fire emissions and atmospheric transport. For example, trajectories frequently pass over southern Sumatra in July but fire emissions from this region are relatively small during this month compared with emissions during August to October. In November, when there are fires in Indonesian Borneo, trajectories arrive mostly from the northeast over the sea and do not pass over land, resulting in a relatively small amount of emissions transported to Singapore in this month (Figure 5).

References

Andela, N., Kaiser, J.W., Heil, A., van Leeuwen, T.T., van der Werf, G.R., Wooster, M.J., Remy, S. and Schultz, M.G.: Assessment of the Global Fire Assimilation System (GFASv1), MACC-II Project Report, 2013.

Arnold, S.R., Chipperfield, M.P., and Blitz, M.A.: A three dimensional model study of the effect of new temperature dependent quantum yields for acetone photolysis, J. Geophys. Res., 110, D22305, doi:10.1029/2005JD005998, 2005.

Arnold, S.R., Spracklen, D.V., Gebhardt, S., Custer, T., Williams, J., Peeken, I. and Alvain, S.: Relationships between atmospheric organic compounds and air-mass exposure to marine biology. Envir. Chem., 7(3), 232-241, 2010.

Balasubramanian, R., Qian, W.-B., Decesari, S.M.C., Facchini, M.C. and Fuzzi, S.: Comprehensive characterization of PM2.5 aerosols in Singapore, J. Geophys. Res., 108 (D16), 4523. http://dx.doi.org/10.1029/2002JD002517, 2003.

Bellouin, N., Rae, J., Jones, A. Johnson, C., Haywood, J. and Boucher, O.: Aerosol forcing in the Climate Model Intercomparison Project (CMIP5) simulations by HadGEM2-ES and the role of ammonium nitrate, J. Geophys. Res., 116, D20206, doi:10.1029/2011JD016074, 2011.

Chew, B., Campbell, J., Reid, J., Giles, D., Welton, E., Salinas, S., and Liew, S.: Tropical cirrus cloud contamination in sun photometer data, Atmos. Environ., 45, 6724–6731, 2011.

Chipperfield, M. P.: New version of the TOMCAT/SLIMCAT offline chemical transport model: Intercomparison of stratospheric tracer experiments, Q. J. Roy. Meteor. Soc., 132, 1179–1203, 2006.

Dentener, F., Kinne, S., Bond, T., Boucher, O., Cofala, J., Generoso, S., Ginoux, P., Gong, S., Hoelzemann, J.J., Ito, A., Marelli, L., Penner, J.E., Putaud, J.-P., Textor, C., Schulz, M., van der Werf, G.R., and Wilson, J.: Emissions of primary aerosol and precursor gases in the years 2000 and 1750 prescribed data-sets for AeroCom, Atmos. Chem. Phys., 6, 4321–4344, doi:10.5194/acp-6-4321-2006, 2006.

Engling, G., He, J., Betha, R., and Balasubramanian, R.: Assessing the regional impact of Indonesian biomass burning emissions based on organic molecular tracers and chemical mass balance modeling, Atmos. Chem. Phys. Discuss., 14, 2773-2798, doi:10.5194/acpd-14-2773-2014, 2014.

Grainger, R.G., Lucas, J., Thomas, G.E. and Ewen, G.B.L.: Calculation of Mie Derivatives, Appl. Opt. 43, 5386. doi:10.1364/AO.43.005386, 2004.

Huang, J., Hsu, N., Tsay, S.-C., Jeong, M.-J., Holben, B., Berkoff, T., and Welton, E.: Susceptibility of aerosol optical thickness retrievals to thin cirrus contamination during the BASE-ASIA campaign, J. Geophys. Res., 116, D08214, doi:10.1029/2010JD014910, 2011.

Ilahi, A. F. and Nurhayati: Characteristic and climatology of pollutant PM10 at Bukit Kototabang, Megasains (ISSN 2086-5589), 3 (3), 138-153, 2012.

Lamarque, J.-F., Bond, T.C., Eyring, V., Granier, C., Heil, A., Klimont, Z., Lee, D., Liousse, D., Mieville, A., Owen, B., Schultz, M.G., Shindell, D., Smith, S.J., Stehfest, E., Van Aardenne, J., Cooper, O.R., Kainuma, M., Mahowald, N., McConnell, J.R., Naik, V., Riahi, K., and van Vuuren, D.P.: Historical (1850-2000) gridded anthropogenic and biomass burning emissions of ozone and aerosol precursors: methodology and application. Atmos. Chem. Phys., 10, 7017–7039, doi:10.5194/acp-10-7017-2010, 2010.

Mann, G.W., Carslaw, K.S., Spracklen, D.V., Ridley, D.A., Manktelow, P.T., Chipperfield, M.P., Pickering, S.J., and Johnson, C.E.: Description and evaluation of GLOMAP-mode: a modal global aerosol microphysics model for the UKCA composition-climate model, Geosci. Model Dev., 3, 519-551, doi:10.5194/gmd-3-519-2010, 2010.

Olson, D.M., Dinerstein, E., Wikramanayake, E.D., Burgess, N.D., Powell, G.V.N., Underwood, E.C., D'Amico, J.A., Itoua, I., Strand, H.E., Morrison, J. C., Loucks, C. J. , Allnutt, T.F., Ricketts, T.H., Kura, Y., Lamoreux, J.F., Wettengel, W.W., Heda, P. and Kassem, K.R.: Terrestrial ecoregions of the

world a new map of life on earth, Bioscience, 51, 933-938, 2001.

Saji, N.H., Goswami, B.N., Vinayachandran, P.N., and Yamagata, T.: A dipole mode in the tropical Indian Ocean, Nature, 401, 360-363, 1999.

Spracklen, D.V., Pringle, K.J., Carslaw, K.S., Chipperfield, M.P., and Mann, G.W.: A global off-line model of size-resolved aerosol microphysics: I. Model development and prediction of aerosol properties, Atmos. Chem. Phys., 5, 2227-2252, doi:10.5194/acp-5-2227-2005, 2005.

Stokes, R.H. and Robinson, R.A.: Interactions in aqueous nonelectrolyte solutions. I. Solute-solvent equilibria, J. Phys. Chem., 70 (7), 2126-2131, 1966.

van der Werf, G.R., Randerson, J.T., Collatz, G.J., Giglio, L., Kasibhatla, P.S., Arellano, A.F., Olsen, S.C., Kasischke, E.S.: Continental-scale partitioning of fire emissions during the 1997 to 2001 El Nino/La Nina period, Science, 303, doi:10.1126/science.1090753, 2004.

van der Werf, G.R., Randerson, J.T., Giglio, L., Collatz, G.J., Kasibhatla, P.S., Arellano, A.F.: Interannual variability in global biomass burning emissions from 1997 to 2004, Atmos. Chem. Phys., 6, doi:10.5194/acp-6-3423-2006, 2006.

van der Werf, G.R., Randerson, J.T., Giglio, L., Collatz, G.J., Mu, M., Kasibhatla, P.S., Morton, D.C., DeFries, R.S., Jin, Y., van Leeuwen, T.T.: Global fire emissions and the contribution of deforestation, savanna, forest, agricultural, and peat fires (1997-2009), Atmos. Chem. Phys., 10, doi:10.5194/acp-10-11707-2010, 2010.

Wiedinmyer, C., Akagi, S.K., Yokelson, R.J., Emmons, L.K., Al-Saadi, J.A., Orlando, J.J., and Soja, A.J.: The Fire INventory from NCAR (FINN): a high resolution global model to estimate the emissions from open burning, Geosci. Model Dev., 4, 625-641, doi:10.5194/gmd-4-625-2011, 2011.